Electronic Supplementary Material (ESI) for New Journal of Chemistry.
This journal is © The Royal Society of Chemistry and the Centre National de la Recherche Scientifique 2023

Supporting Information

A novel carbazole-benzothiazole based chemodosimeter for chromogenic and fluorogenic recognition of CN^-

Atanu Maji, Amitav Biswas, Akash Das, Saswati Gharami, Krishnendu Aich and Tapan K. Mondal*

Department of Chemistry, Jadavpur University, Kolkata- 700032, India. E-mail:tapank.mondal@jadavpuruniversity.in

CONTENTS

Fig. S1. ^1H NMR spectrum of CBTA

Fig. S2. ^{13}C NMR spectrum of CBTA

Fig. S3. HRMS spectrum of CBTA

Fig. S4. IR spectrum of CBTA

Fig. S5. Change in UV-Vis spectra of the probe (CBTA) (20 μM) upon gradual addition of 2 equivalent of various anions (40 μM)

Fig. S6. Job's plot of CBTA forCN^-

Fig. S7. Linear response curve of CBTA depending on CN^- ion concentration

Fig. S8. pH study of CBTA for CN^-

Fig. S9. Lifetime decay profile of CBTA and CBTA-CN^-

Figure S10: Photostability study of CBTA and CBTA-CN adduct

Fig. S11. Optimized structure of CBTA calculated by DFT/B3LYP/6-31+G(d) method

Fig. S12. Optimized structure of CBTA-CN^- calculated by DFT/B3LYP/6-31+G(d) method

Fig. S13. Contour plots of some selected molecular orbitals of CBTA

Fig. S14. Contour plots of some selected molecular orbitals of CBTA-CN^-

Fig.S15. Color variations upon addition of different anions (40 μM) to the sensor CBTA (20 μM) under sunlight (a) and 365 nm UV light (b).

Fig. S16. ^1H NMR of CBTA-CN^- adduct

Fig. S17. HRMS of CBTA-CN^- adduct

Fig. S18. Mole ratio plot of CBTA for CN^-

Fig. S19. Chemosensor performance of CBTA in buffer solution

Table S1. Vertical electronic transitions calculated by TDDFT/B3LYP/CPCM method for CBTA and CBTA-CN^- in DMSO.
Table S2: Fluorescence lifetime data
Table S3. Determination of quantum yield (φ) of sensor CBTA at different water fraction (f_w)
Table S4. Sensor CBTA compared to others previously reported receptors

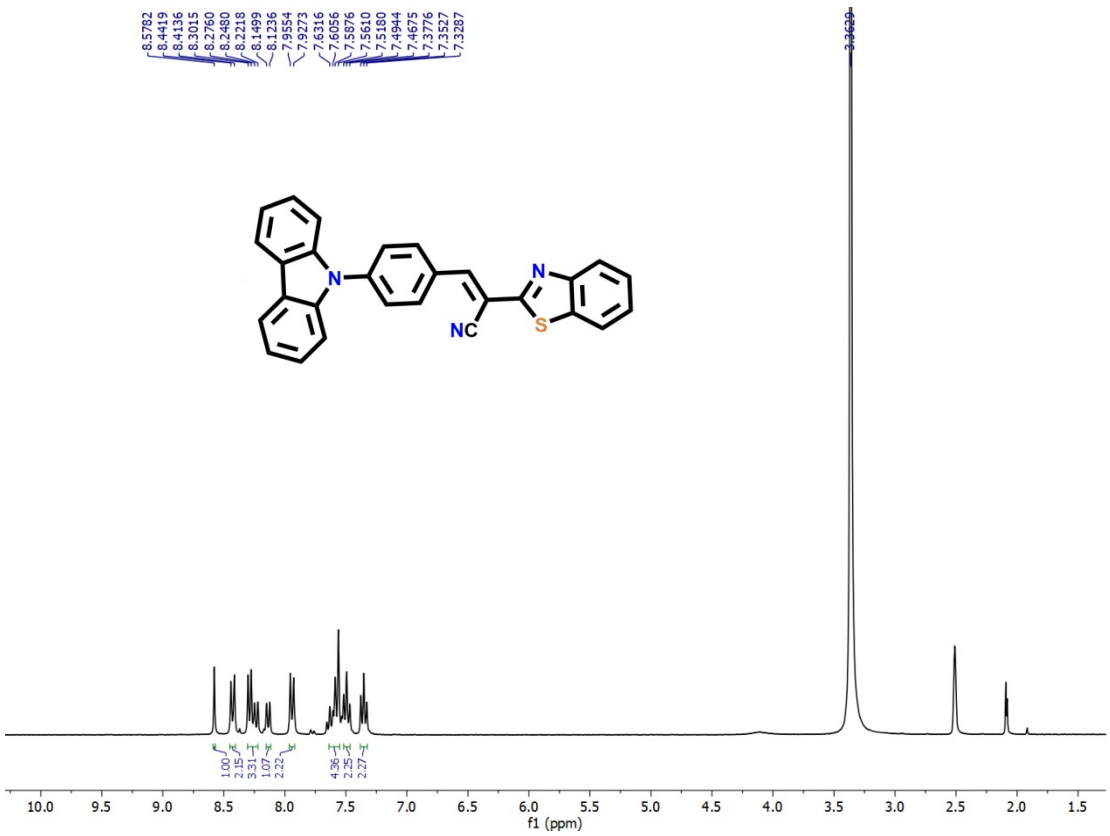

Figure S1: ^{1}H NMR (300 MHz) spectrum of the probe (CBTA) in DMSO-d_6

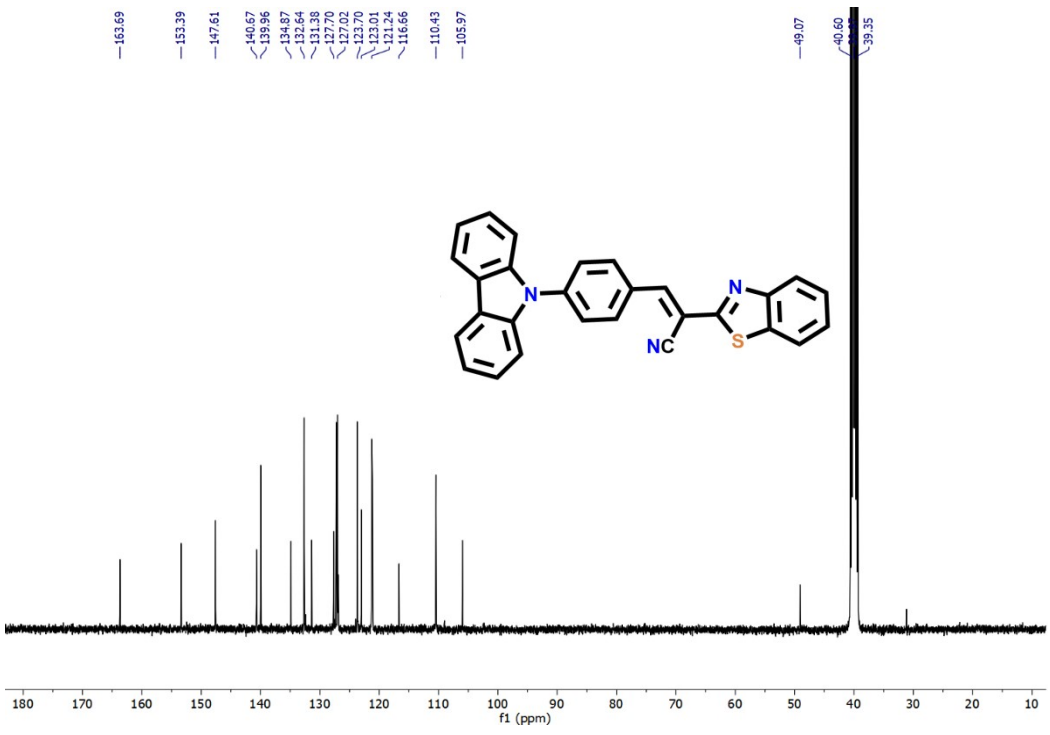

Figure S2: ^{13}C NMR (75 MHz) spectrum of the receptor (CBTA) in DMSO-d_6

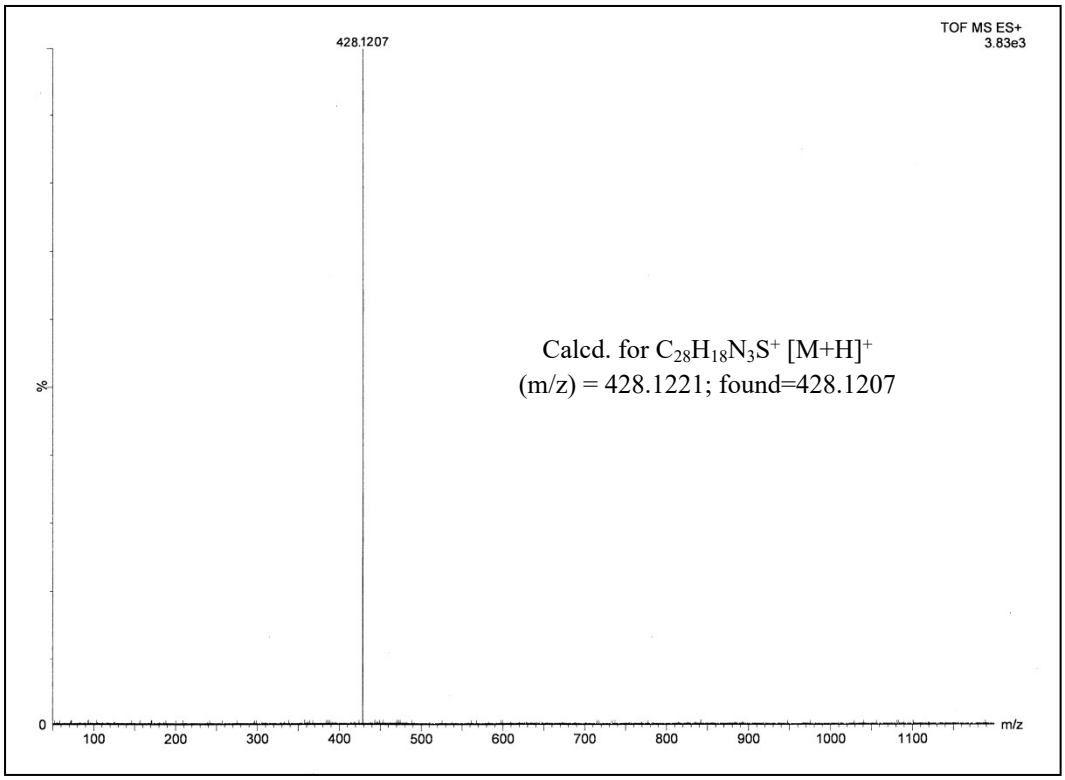

Figure S3: HRMS of the receptor (CBTA)

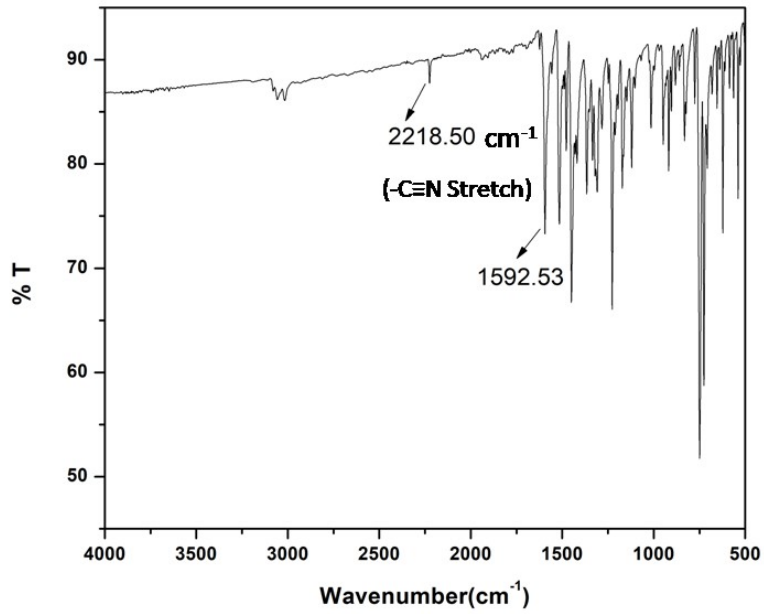

Figure S4: IR Spectrum of CBTA

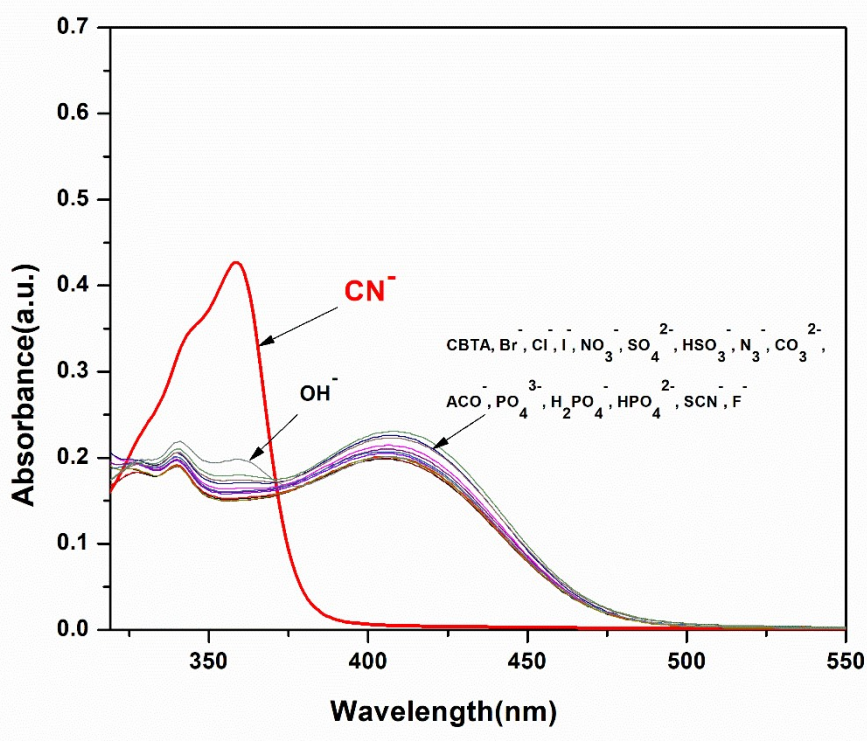

Figure S5: UV-Vis change of CBTA (10 μM) upon addition of different anions, i.e. Br^-, Cl^-, I^-, NO_3^-, SO_4^{2-}, SCN^-, CO_3^{2-}, N_3^-, OH^-, HCO_3^-, $H_2PO_4^-$, HPO_4^{2-}, F^-, ACO^-, $PO_4^{3-}$and CN^- (40 μM) in DMSO/H_2O (40:60, v:v) using HEPES buffered solution at pH=7.2.

Job's Plot

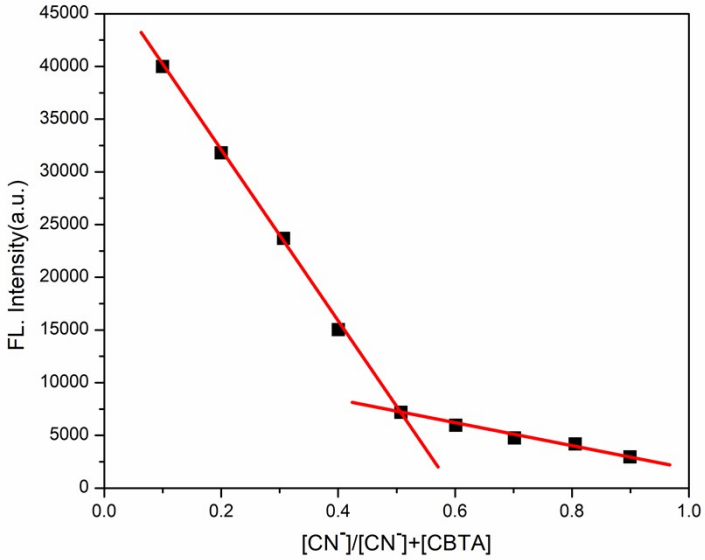

Figure S6: Job's plot of CBTA for CN^-

Determination of detection limit:

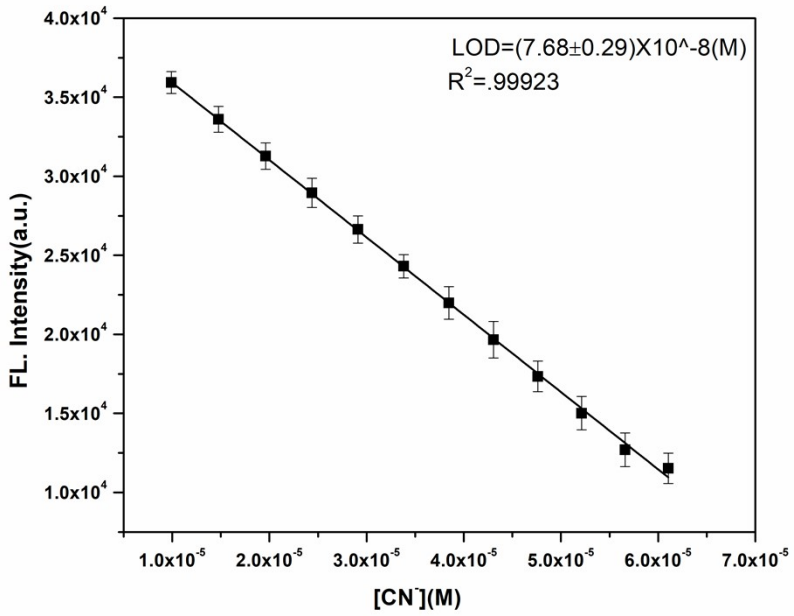

Figure S7: Linear response curve of CBTA at 616 nm depending on the CN^-concentration.

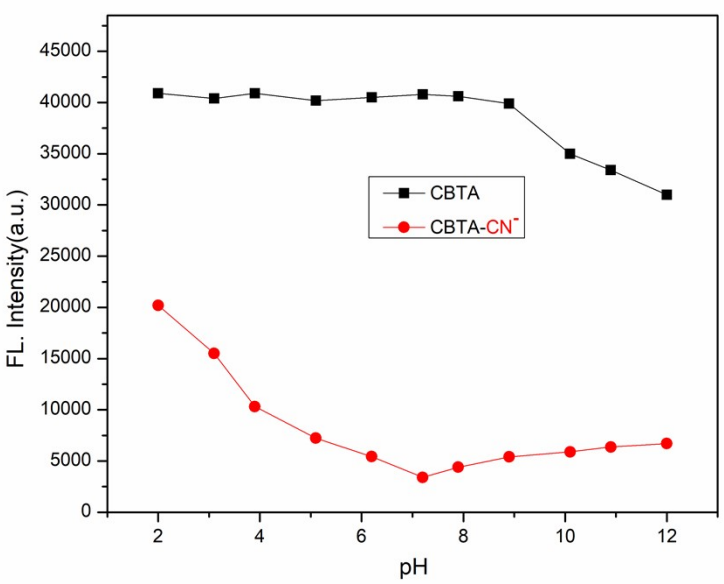

Figure S8: pH study of CBTA for CN^-

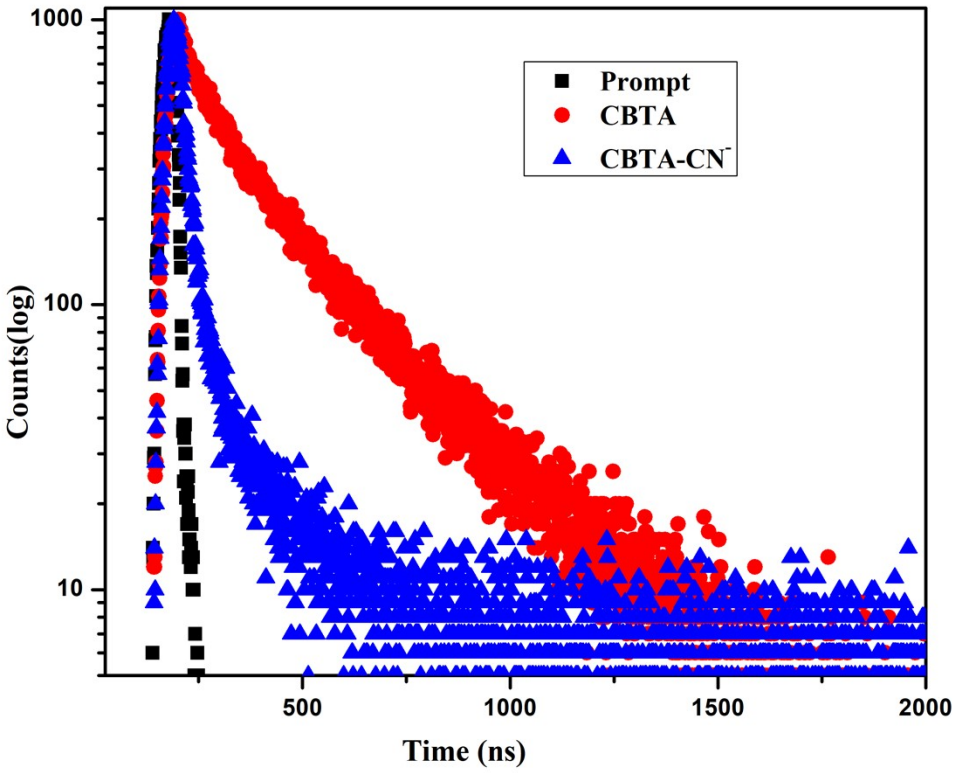

Figure S9: Lifetime decay profile of CBTA and CBTA-CN^- adduct.

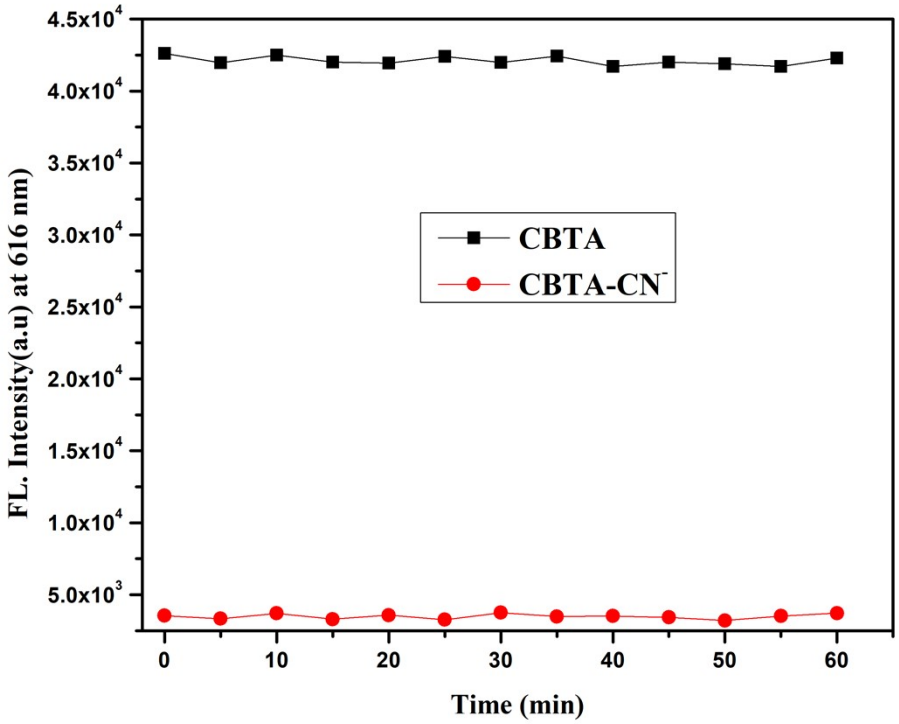

Figure S10: Photostability study of CBTA and CBTA-CN adduct.

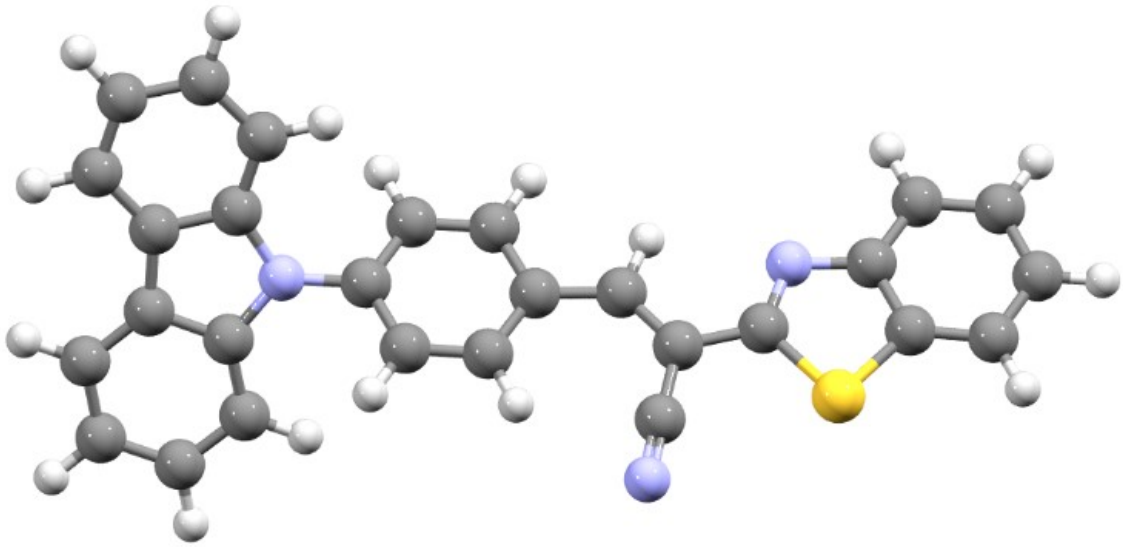

Figure S11. Optimized structure of CBTA calculated by DFT/B3LYP/6-31+G(d) method.

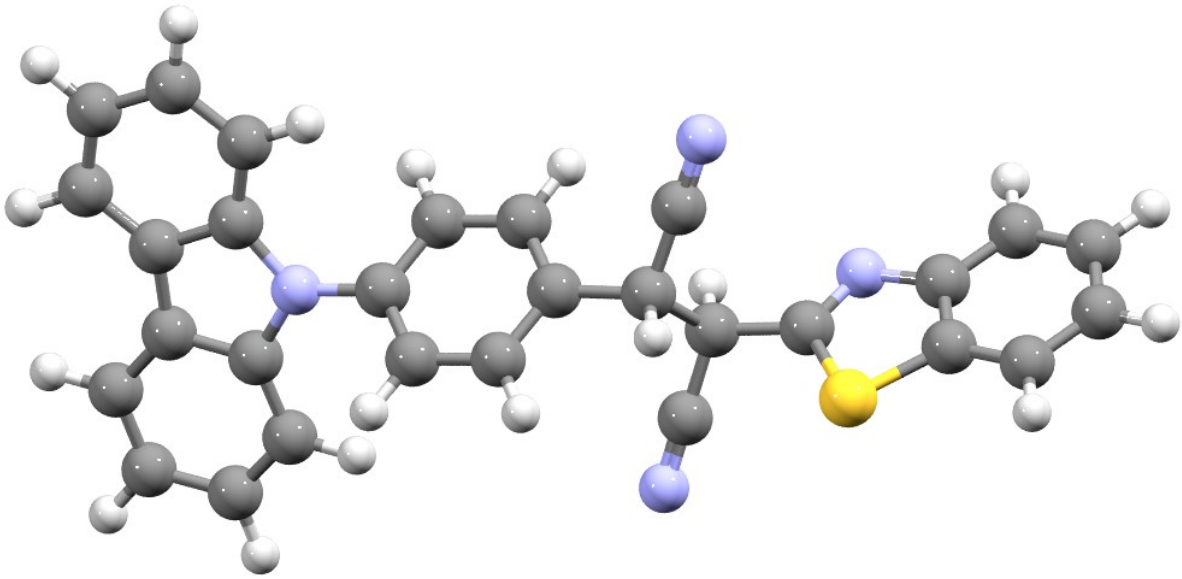

Figure S12. Optimized structure of CBTA-CN^- calculated by DFT/B3LYP/6-31+G(d) method.

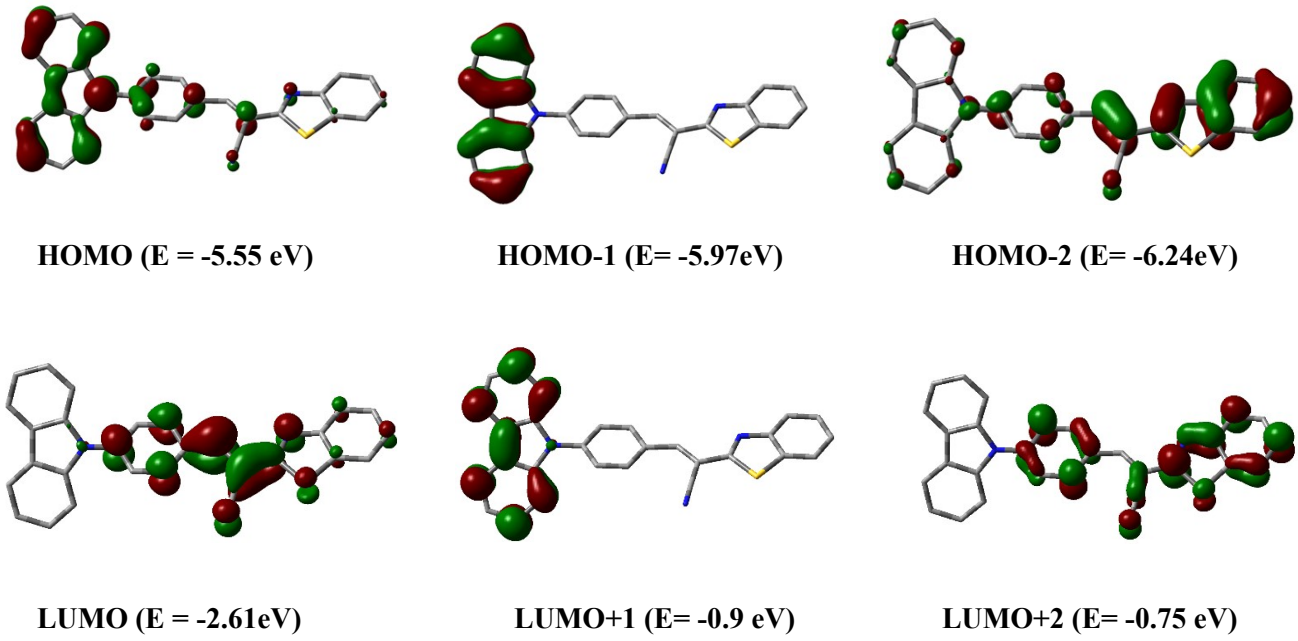

Figure S13. Contour plots of some selected molecular orbitals of CBTA.

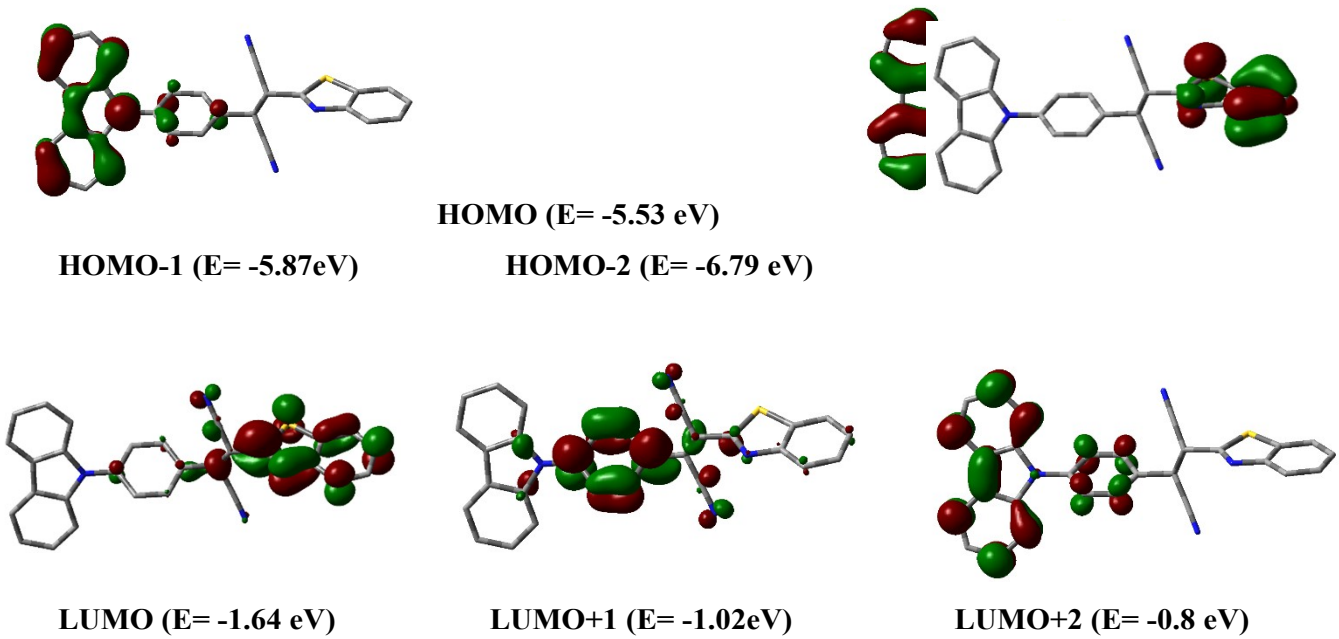

Figure S14. Contour plots of some selected molecular orbitals of CBTA-CN^-

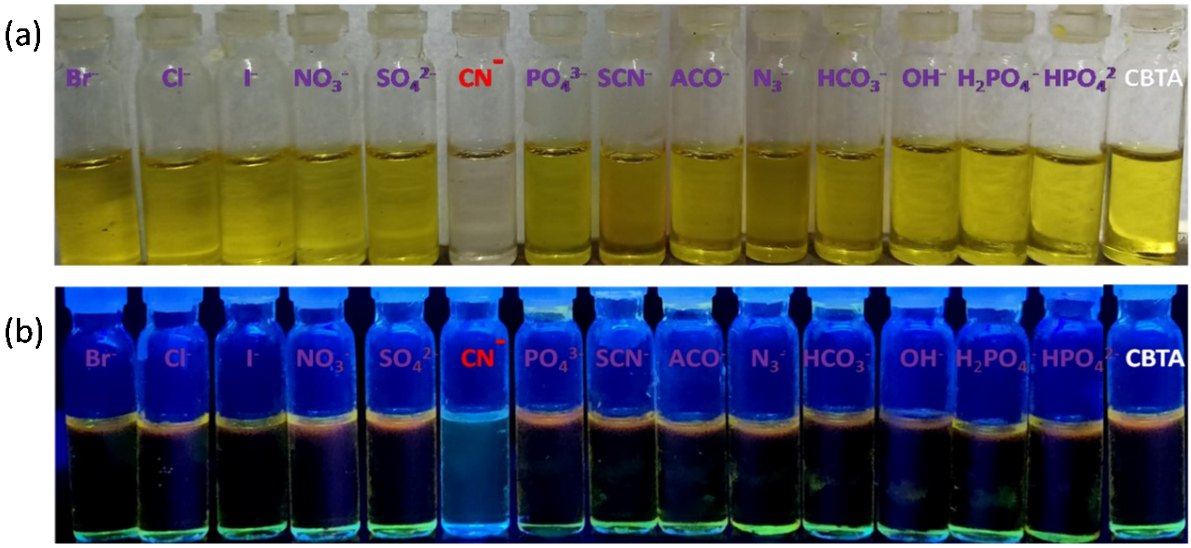

Figure S15: Color variations upon addition of different anions (40μM) to the sensor CBTA (20 μM) under sunlight(a) and under UV light(b).

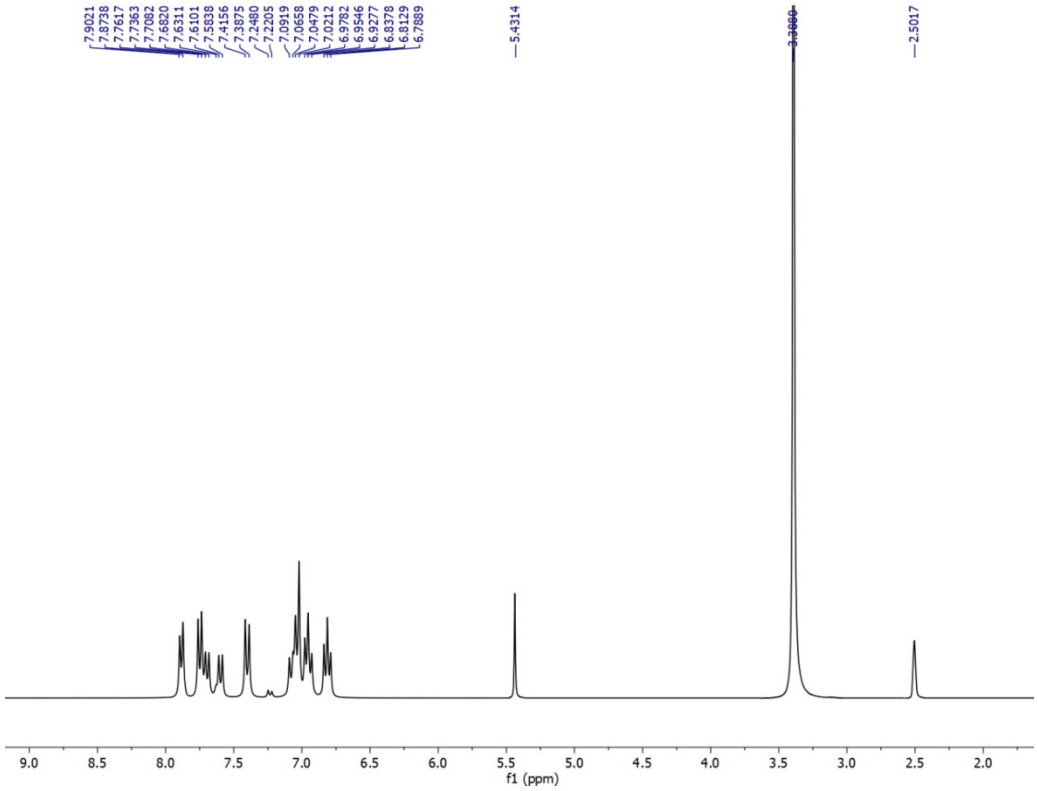

Figure S16: ^{1}H NMR (300 MHz) spectra of the CBTA-CN^- adduct in DMSO-d_6.

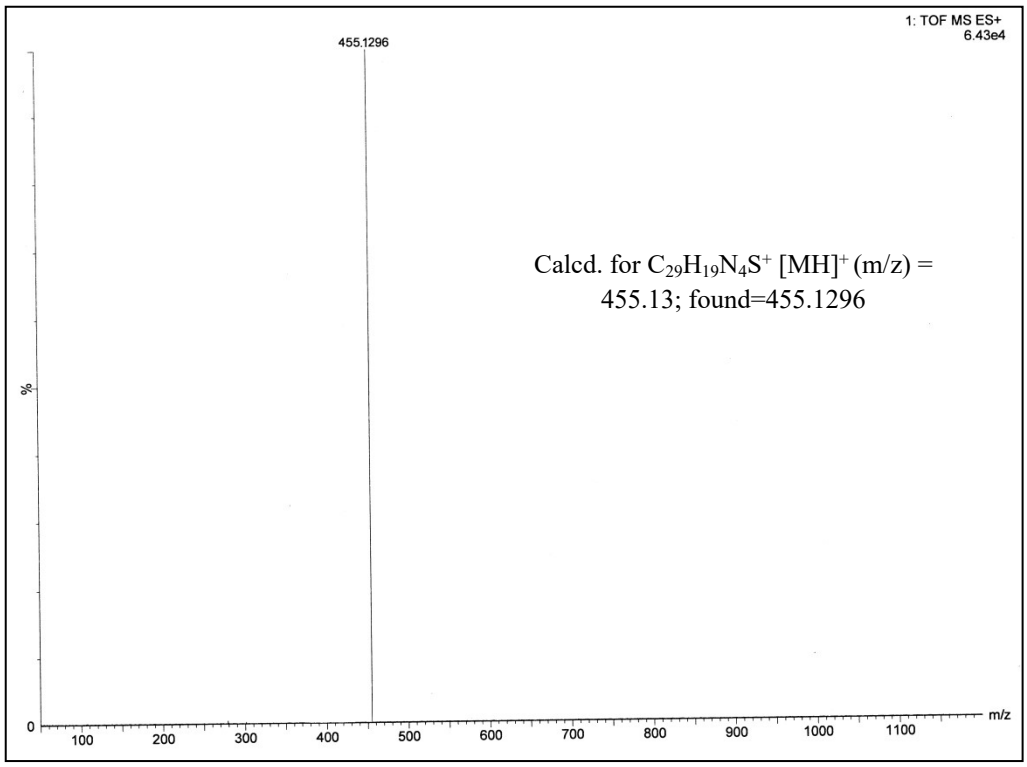

Figure S17: HRMS of the CBTA-CN^- adduct.

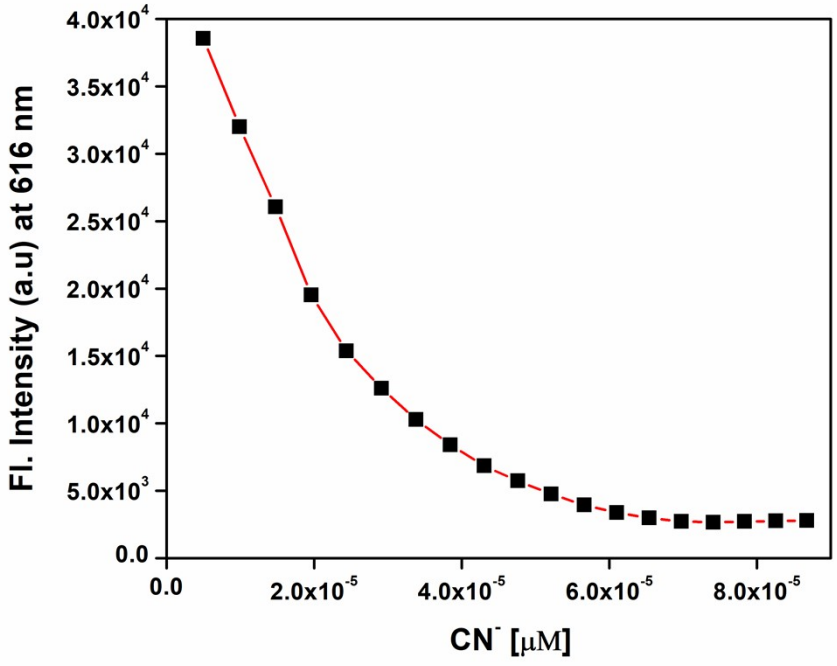

Fig. S18: Mole ratio plot of CBTA for CN^-

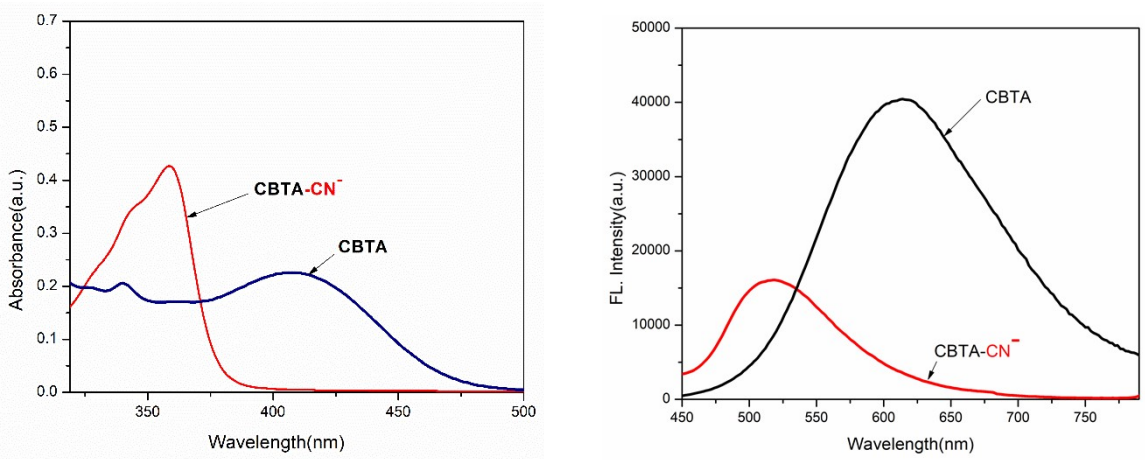

Fig. S19: Chemosensor performance of CBTA in buffer solution

TableS1. Vertical electronic transitions of CBTA and CBTA-CN^- calculated by TDDFT/CPCM method

Compd.	λ (nm)	E (eV)	Osc. Strength (f)	Key excitations
CBTA	491.45	2.5228	0.7330	(99%)HOMO→LUMO
	377.35	3.2857	0.5544	(97%)HOMO-2→LUMO
	293.33	4.2268	0.2105	(85%)HOMO-6→LUMO
	359.31	3.4506	0.0842	(97%)HOMO-3→LUMO
	272.04	4.5576	0.1642	(72%)HOMO-1→LUMO+1
	242.34	5.1161	0.6343	(62%)HOMO→LUMO+6
	231.79	5.3491	0.1404	(41%)HOMO-4→LUMO+1 (35%)HOMO-1→ LUMO+7
CBTA-CN^-	340.06	3.6459	0.1186	(95%)HOMO → LUMO
	308.11	4.0241	0.1946	(51%)HOMO → LUMO+2 (41%) HOMO→LUMO+1
	260.43	4.7608	0.4729	(84%)HOMO-3 → LUMO
	243.46	5.0926	0.1665	(63%)HOMO-4 → LUMO
	240.62	5.1528	0.4896	(27%)HOMO-4 → LUMO (46%)HOMO → LUMO-7
	214.97	5.7675	0.1842	(26%)HOMO-5→ LUMO+1 (19%)HOMO-3 → LUMO+3 (25%)HOMO→ LUMO+10

Determination of fluorescence Quantum Yields (Φ) of CBTA and its complex with CN^-

The luminescence quantum yield was determined using coumarin-153 as reference dye. The compounds and the reference dye were excited at the similar wavelength and the emission spectra were then studied. The area of the emission spectrum was integrated and the quantum yield is determind according to the following equation:

$\phi_S/\phi_R = [A_S/A_R] \times [(Abs)_R/(Abs)_S] \times [n_S^2/n_R^2]$

Here, ϕ_S and ϕ_R are the luminescence quantum yields of the sample and reference dye, respectively. A_S and A_R are the area under the emission spectra of the sample and the reference respectively, $(Abs)_S$ and $(Abs)_R$ are the respective optical densities of the sample and the reference solution at the wavelength of excitation, and n_S and n_R stand for the values of refractive index for the respective solvent used for the sample and reference.

The quantum yields of CBTA and CBTA-CN are determined using the above mentioned equation and the values are found to be 0.205 and 0.015 respectively.

Table S2: Fluorescence lifetime data

DMSO(Solvent)	Quantum yield(φ)	τ(ns)	$K_r(10^8 \times S^{-1})$	$K_{nr}(10^8 \times S^{-1}$
CBTA	0.205	6.1	0.336	1.303
CBTA-CN$^-$	0.015	1.38	0.1086	7.137

Table S3: Determination of quantum yield (φ) of sensor CBTA at different water fraction (f_w)

Sensor	DMSO:H_20 (v/v)	Water fraction(f_w)	Quantum Yields(φ)
CBTA	100:0	0%	0.07
	60:40	40%	0.081
	50:50	50%	0.146
	40:60	60%	0.205
	30:70	70%	0.184
	20:80	80%	0.131
	10:90	90%	0.082

Table S4: Sensor CBTA towards CN^- compared to others previously reported receptors

Probe	Solvent System	Detection limit	Reaction time	Reference
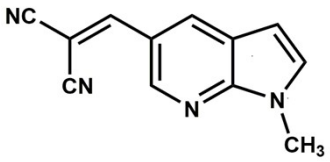	THF/H_2O(9:1)	2×10^{-6} M		[1]
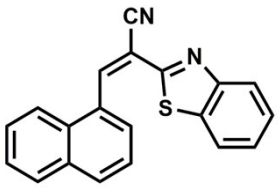	DMF	0.07 μM		[2]
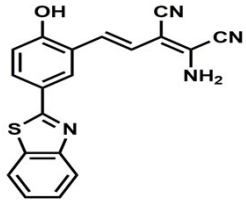	DMSO/H_2O (7:3)	1.4×10^{-7} M		[3]
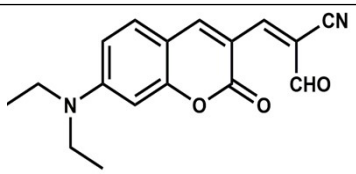	CH_3CN	0.328μM		[4]

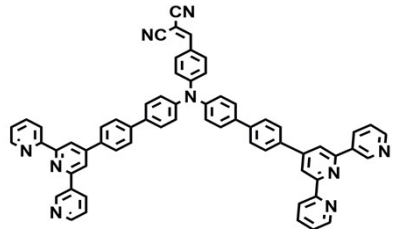	H_2O/THF(9:1)	3.83×10^{-6} M		[5]
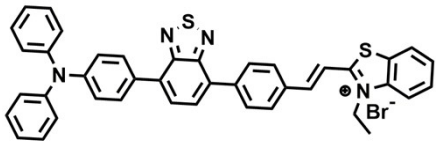	H_2O/THF(8:2)	1.3×10^{-7} M		[6]
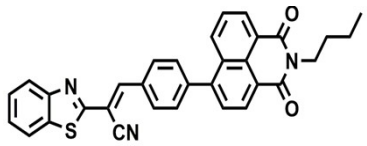	THF	0.034 μM		[7]
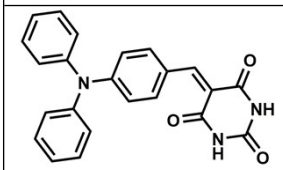	DMSO/H_2O (1:99)	2.95×10^{-8} M		[8]
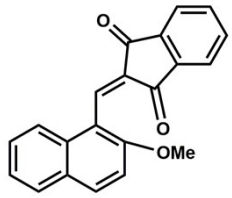	H_2O-DMF (9:1,v/v)	1.15-1.2 nM	10-30 sec	[9]
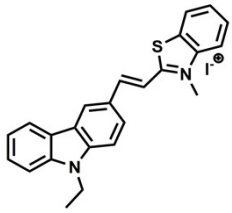	DMSO	0.94 μM		[10]
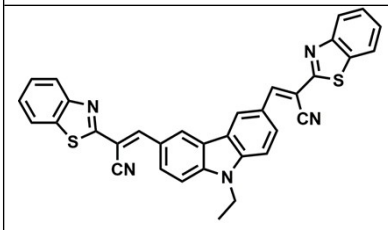	DMSO-H_2O (4/1,v/v)	3.75 nM	9-10 min	[11]

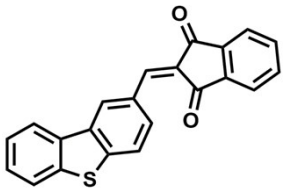	DMSO/H_2O (1:99,v/v)	2.26×10^{-7}M	15 sec	[12]
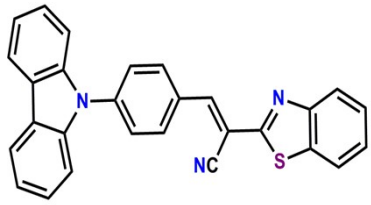	DMSO/H_2O (40:60,v/v)	7.68×10^{-8} M	22 sec	This work

References

1. K. Y. Chen and W. C. Lin, *Dyes Pigm.*, 2015, **123**, 1-7.
2. K. W. Kulig, Cyanide Toxicity, U.S. Department of Health and Human Services, Atlanta GA, 1991.
3. S. Malkondu, S. Erdemirand, S. Karakurt, *Dyes Pigm.*, 2020,**174**,108019.
4. L. Yuan, W. Lin, Y. Yang, J. Song and J. Wang, *Org. Lett.*, 2011, **13,** 3730-3733.
5. Y. Li, Z. Gu, T. He, X. Yuan, Y. Zhang, Z. Xu, H. Qiu, Q. Zhang and S. Yin, *Dyes Pigm.*, 2020, **173**, 107969.
6. B. Zhai, Z. Hu, C. Peng, B. Liu, W. Li and C. Gao, *Spectrochim. Acta A.*, 2020, **224,** 117409.
7. T. S. Reddy, H. Moon and M. S. Choi, *Spectrochim Acta A.*,2021, **252**, 119535.
8. B. Zuo, L. Liu, X. Feng, D. Li, W. Li, M. Li, M. Huang and Q. Deng, *Dyes Pigm.*, 2021, **193**, 109534
9. N. Maurya and A. K. Singh, *Sens. and Actuat. B Chem.*, 2017, **245**, 74–80.
10. J. Chao, Z. Li, Y. Zhang, F. Huo, C. Yin, Y. Liu, Y. Li and J. Wang, *J. Mater. Chem.B.*, 2016, **4**, 3703-3712.
11. L. Patra, K. Aich, S. Gharami and T. K. Mondal, *J. Lumin.*, 2018, **201**, 419-426
12. Q. Zou, J. Du, C. Gu, D. Zhang, F. Tao and Y. Cui, *J. Photochem. Photobiol. A. Chem.*, 2021, **405**, 112993